

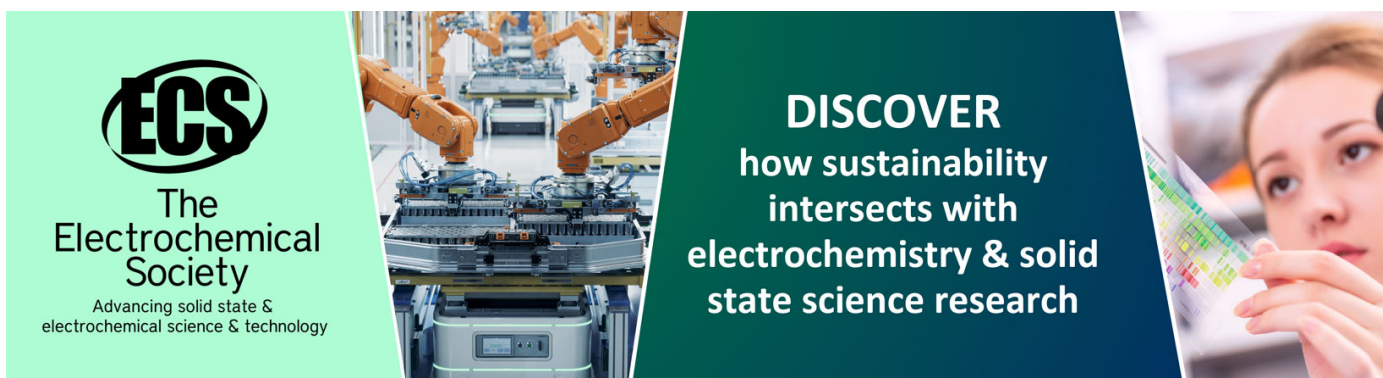
## The experimental validation of a new energy harvesting system based on the wake galloping phenomenon

To cite this article: Hyung-Jo Jung and Seung-Woo Lee 2011 *Smart Mater. Struct.* **20** 055022

View the [article online](#) for updates and enhancements.

### You may also like

- [Piezoelectric wind energy harvesting subjected to the conjunction of vortex-induced vibration and galloping: comprehensive parametric study and optimization](#)  
Kai Yang, Kewei Su, Junlei Wang et al.
- [Modeling and experimental investigation of asymmetric distance with magnetic coupling based on galloping piezoelectric energy harvester](#)  
Huirong Zhang, Leian Zhang, Yuanbo Wang et al.
- [Coupled electro-aeroelastic energy harvester model based on piezoelectric transducers. VIV-galloping interaction and nonlinear switching circuits](#)  
Emiliano Del Priore, Giovanni Paolo Romano and Luca Lampani



**ECS**  
The  
Electrochemical  
Society  
Advancing solid state &  
electrochemical science & technology

**DISCOVER**  
how sustainability  
intersects with  
electrochemistry & solid  
state science research

# The experimental validation of a new energy harvesting system based on the wake galloping phenomenon

Hyung-Jo Jung<sup>1,3</sup> and Seung-Woo Lee<sup>1,2</sup>

<sup>1</sup> Department of Civil and Environmental Engineering, KAIST, Daejeon 305-701, Korea

<sup>2</sup> TE Solution Co. Ltd, Gyeonggi-do 456-825, Korea

E-mail: [hjung@kaist.ac.kr](mailto:hjung@kaist.ac.kr)

Received 19 October 2010, in final form 21 March 2011

Published 27 April 2011

Online at [stacks.iop.org/SMS/20/055022](http://stacks.iop.org/SMS/20/055022)

## Abstract

In this paper, a new energy harvesting system based on wind energy is investigated. To this end, the characteristics and mechanisms of various aerodynamic instability phenomena are first examined and the most appropriate one (i.e. wake galloping) is selected. Then, a wind tunnel test is carried out in order to understand the occurrence conditions of the wake galloping phenomenon more clearly. Based on the test results, a prototype electromagnetic energy harvesting device is designed and manufactured. The effectiveness of the proposed energy harvesting system is extensively examined via a series of wind tunnel tests with the prototype device. Test results show that electricity of about 370 mW can be generated under a wind speed of  $4.5 \text{ m s}^{-1}$  by the proposed energy harvesting device. The generated power can easily be increased by simply increasing the number of electromagnetic parts in a vibrating structure. Also, the possibility of civil engineering applications is discussed. It is concluded from the test results and discussion that the proposed device is an efficient, economic and reliable energy harvesting system and could be applied to civil engineering structures.

(Some figures in this article are in colour only in the electronic version)

## 1. Introduction

When a structure is subjected to wind loads, the structure may experience unwanted, excessive vibrations due to aerodynamic instability phenomena such as vortex-induced vibration, galloping, flutter and buffeting. In the fields of civil and aerospace engineering, these kinds of vibrations of a structure have been generally considered as ones to be avoided. For example, the old Tacoma Narrows Bridge in the United States collapsed due to one of these aerodynamic instability phenomena (i.e. the torsional flutter) in 1940. Since then, aerodynamic instability has become a major concern to be carefully examined during the design of a structure, especially a long-span structure such as a cable-supported bridge or a high-rise building.

From a totally different perspective, these aerodynamic instability phenomena might be considered as a new energy

source for an alternative energy harvesting device based on wind power. That is, electrical energy can be generated by making use of the divergent vibration characteristics of these phenomena which can destroy massive structures such as bridges. The possibility of this idea was first addressed by Duncan in 1948 [1]. In the early 1980s, McKinney and DeLaurier [2] proposed a prototype energy power generating device based on the flutter phenomenon. They carried out wind tunnel tests and demonstrated that their device was comparable to a conventional windmill. In 1999, Jones *et al* [3] described their numerical and experimental methods for an oscillating-wing generator and compared the efficiencies of their system to those of McKinney and DeLaurier. In 2003, Isogai *et al* [4] proposed a different type of energy harvesting device using a flapping wing under the flutter phenomenon. They introduced an electric motor to mechanically drive the pitching oscillation of the whole wing, resulting in the increased efficiency of the system. Recently, Ertuk *et al* [5, 6] reported the use of a curved airfoil section with piezoceramics for energy harvesting with

<sup>3</sup> Author to whom any correspondence should be addressed.

mathematical modeling as well as experimental validations, and Bryant and Garcia [7, 8] discussed energy harvesting from aeroelastic vibrations using an airfoil section attached to a cantilever, both theoretically and experimentally. All of the studies mentioned previously were focused on flapping-wing-type power generators based on the flutter phenomenon, which could be inspired from oscillating wings in an aircraft.

Dickson [9] and Li and Lipson [10] suggested a bio-inspired piezo-leaf-based wind energy harvesting configuration and demonstrated an initial design. Also, Li *et al* [11] explored a dangling cross-flow stalk arrangement, which can amplify the vibration by an order of magnitude. They claimed that their architecture makes it appropriate for low-cost organic piezo-materials. A concept for microwind power generation using flow-induced self-excited oscillations of a piezoelectric beam embedded within a cavity, which is inspired by music-playing harmonicas, was proposed by St Clair *et al* [12]. They emphasized that their device can eliminate the bandwidth issues associated with resonant vibratory energy harvesters.

In the field of civil engineering, similar research inspired by the divergent oscillation of some parts of bridges under wind loads was carried out in the mid-1990s. Matsumoto and his colleagues [13, 14] examined the applicability of a rectangular section to flutter-based power generation focusing on the amplitude ratios between heaving and torsional motions. They showed from the wind tunnel test that a more bluff rectangular section had the advantage of flutter generation, and that higher efficiency can be obtained on the resonance condition. As above, some research has been carried out for developing an energy harvesting system based on aerodynamic instability phenomena, more specifically divergent oscillation due to the flutter phenomenon. It is known that the efficiency of the flutter-based energy harvesting system can dramatically improve with increasing wind speed. On the other hand, it has several disadvantages such as the drastic deterioration of efficiency in the range of low wind speeds and the significant reduction of the stability of the system under unexpected wind speeds (i.e. a gust of wind). Moreover, it is not easy to control divergent oscillations because their amplitudes may increase drastically according to an increase in wind speed. Therefore, it is difficult to steadily obtain electrical energy in the condition of variable wind speed using divergent oscillations.

Recently, Jung *et al* [15] proposed a new class of energy harvesting devices based on the wake galloping phenomenon, which is one of the aerodynamic instability phenomena and which may occur in a closely spaced pair of circular cylinders in a tandem arrangement, such as the cables of bridges or power transmission lines in wind [16]. They claimed that their device could solve the above-mentioned difficulties and verified the feasibility of their method by producing preliminary experimental results. However, they did not provide any details on the reasons why they chose wake galloping among several phenomena or the operating principle of the proposed energy harvesting system. Also, the experimental test results for the validation of the proposed system were very limited and the discussion was superficial. The estimation process of the generated power from the energy harvesting device was not clear and needs to be modified.

Moreover, the applicability of the system to civil engineering structures was not taken into account. Therefore, a more detailed investigation should follow their conceptual study in order to more clearly validate the effectiveness of the wake-galloping-based energy harvesting system.

This paper presents the results of an extensive experimental investigation to validate the applicability of the wake-galloping-based electromagnetic energy harvesting device. To do this, the characteristics and mechanisms of various aerodynamic instabilities are examined first. Then, a wind tunnel test is carried out in order to more clearly understand the occurrence condition of the selected aerodynamic instability phenomenon (i.e. wake galloping). Based on the wind tunnel test results, a prototype electromagnetic energy harvesting device is designed and manufactured. By using the prototype device, the effectiveness of the proposed system is verified with different parameters through the wind tunnel test. Its applicability to civil engineering structures is also carefully discussed based on the wind data measured at the bridge site.

## 2. Characterization test of wake galloping phenomenon

### 2.1. Review of various aerodynamic instability phenomena

In this section, the characteristics of various aerodynamic instability phenomena, such as vortex-induced vibration, divergent oscillations (e.g. galloping, flutter, etc), wake galloping and the buffeting response, are briefly introduced in order to carefully select an appropriate phenomenon for energy harvesting purposes. Figure 1 shows the typical velocity–amplitude curves of the aerodynamic instability phenomena.

**2.1.1. Vortex-induced vibration.** This phenomenon is one of the most classical-type aerodynamic instability phenomenon. Vibration with a limited amplitude may occur in a body due to the periodic cross-wind forces arising from the shedding of vortices in the wake of the body. In one or more narrowly limited ranges of wind speed, the exciting frequency may be close enough to one of the natural frequencies of the body to cause resonance and, consequently, cross-wind oscillations. Figure 1(a) represents the typical velocity–amplitude curve for this phenomenon.

**2.1.2. Divergent oscillations such as galloping and flutter.** Divergent oscillations are aerodynamic instability phenomena that can lead to an increase in the magnitude of the oscillatory motions and/or in divergent behavior according to an increase in wind speed (see figure 1(b)). Galloping is a large-amplitude aeroelastic oscillation that can be experienced by cylinders of prisms with certain types of cross section (e.g. rectangular section, D-section). The oscillations occur in a plane normal to the oncoming flow velocity. The flow speeds cause vortex-induced vibration. For galloping to be possible, the steady-state aerodynamic lift coefficient derivatives must be negative. This is known as the Glauert–Den Hartog necessary condition for galloping. The flutter of airfoils is one of the earliest

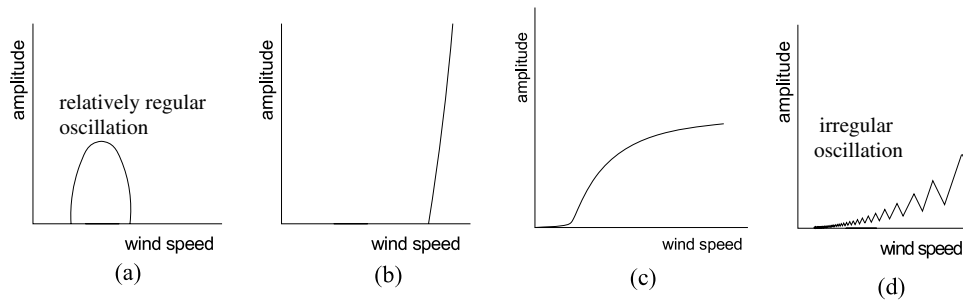


**Figure 1.** Typical velocity–amplitude curves of aerodynamic instability phenomena: (a) vortex-induced vibration, (b) divergent oscillations (i.e. galloping, flutter, coupling flutter), (c) wake galloping and (d) buffeting.

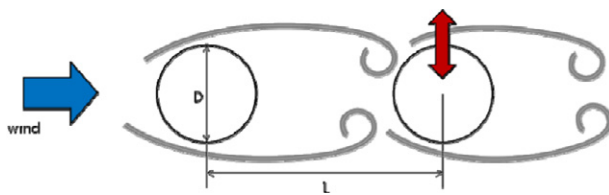


**Figure 2.** Schematic of wake galloping phenomenon.

aeroelastic oscillations. Flutter instability is a divergent-type self-controlled aerodynamic vibration, and the study of this phenomenon was initiated in the field of aeronautics to aerodynamically stabilize airfoils. After the Tacoma Narrows Bridge accident in 1940, the flutter instability of bridge decks of long-span bridges has become a major concern in their design.

**2.1.3. Wake galloping.** Wake galloping is known to occur in parallel cylinders because of wakes from the windward cylinder. Figure 2 shows the schematic of this phenomenon. The vibration orbit depends upon the arrangement of parallel cylinders, and the appearance of vibration is limited to a spatial range. According to Matsumoto [13, 14], if the distance between two cables is larger than approximately six times the cable diameter, then the vibration does not appear. The joining devices of two cylinders are often used for vibration control, but some of them have been damaged because of the large energy of this exciting force. Figure 1(c) represents the typical velocity–amplitude curve in the case of wake galloping.

**2.1.4. Buffeting response.** The vibration of structures induced by oncoming turbulence or the turbulence generated by its own structure is called buffeting, which is a kind of random vibration. The buffeting response irregularly increases gradually with wind speed, as shown in figure 1(d). In the 1940s and 1950s, this phenomenon had been studied mainly in the aeronautical field and Davenport [17] summarized the evaluation methods of the buffeting of buildings and long-span bridges by the use of a stochastic process. His evaluation methods of the buffeting forces or buffeting response have been widely used in wind-resistant design codes for buildings and bridge structures throughout the world.

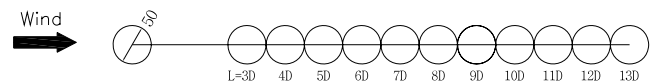


**Figure 3.** Definition of the interval between parallel cylinders.

**2.1.5. The selection of an appropriate aerodynamic instability phenomenon for energy harvesting.** In recent years, alternative approaches for replacing conventional blade-type wind power systems have been investigated by focusing on aerodynamic divergent oscillations such as galloping, flutter and coupling flutter [1–8, 13, 14]. However, the onset speeds of divergent oscillations are not relatively low and their amplitudes may increase drastically with an increase in wind speed. Therefore, harvesting energy steadily in conditions of variable wind speed using divergent oscillations is difficult. On the other hand, vortex-induced vibration may occur at relatively low wind speed. However, it occurs only within a very narrow range of wind speed along with a relatively small amplitude. Therefore, an energy harvesting system using vortex-induced vibration may be inefficient.

In comparison to divergent oscillations and vortex-induced vibration, a different type of aerodynamic instability phenomenon, wake galloping, may be appropriate for an energy harvesting system since it may occur at relatively low wind speeds and has a wide range of wind speeds with large but finite amplitude [15]. The characteristics of the wake galloping phenomenon should be more carefully investigated for use in energy harvesting.

## 2.2. Test set-up

To analyze the occurrence conditions and vibration characteristics of the wake galloping phenomenon, the characteristics of two cylinders with variations of the distance between their centers and characteristics with different wind directions are investigated. Figure 3 shows the schematic of the test.

The dimensions of the wind tunnel used in this test are shown in figure 4. The size of the test section is 1 m wide, 1.5 m high and 6 m long. The range of wind speeds is 0–22.5 m s<sup>−1</sup>. An optical-type displacement sensor that can measure the horizontal displacement and the vertical displacement simultaneously is used for the vibration test.

The wind tunnel tests are carried out in a smooth flow condition and the range of wind speeds is 0–18 m s<sup>−1</sup>. The



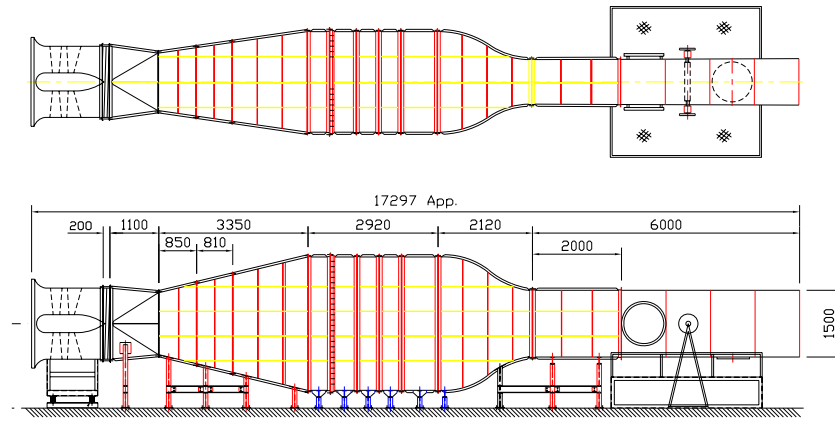


Figure 4. Wind tunnel facility.

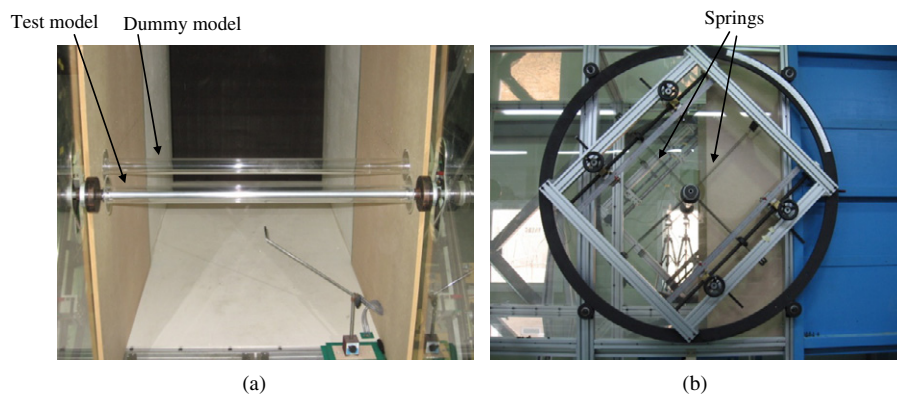


Figure 5. Experimental set-up; (a) tandem arrangement and (b) elastic mounting system using springs.

Table 1. Data of test model.

Diameter	Length	Mass per length	Natural frequency	Logarithmic decrement	Scruton number
5 cm	0.85 m	8.184 kg m <sup>-1</sup>	1.56 Hz	$\delta = 0.006$	32.0

experimental set-up for the test is shown in figure 5. As seen from the figure, two parallel cylinder models of the same size ( $D = 50$  mm) are used. A dummy model, which is placed on the windward side, cannot be vibrated because it is fixed at both ends and a test model, which is placed in the leeward side, is suspended by the elastic mounting system using springs (see figure 5(b)). This system allows the vertical and horizontal motions of a downstream cylinder (i.e. the test model) with a very small damping ratio (i.e. the logarithmic decrement of 0.006). In the test, there exist the inertia force from the cylinders, the aerodynamic force due to the wind and the restoring force from the elastic mounting system. The geometric and dynamic properties of the test model are listed in table 1. The center-to-center spacings of the models are  $3D$ – $13D$  and the tests are carried out at intervals of  $1D$ . The Scruton number ( $S_c$ ) of the test model is listed in table 1 ( $S_c = (2m\delta)/(\rho D^2)$ ,  $m$ : mass per length,  $\delta$ : logarithmic damping,  $\rho$ : air density,  $D$ : cylinder diameter).

### 2.3. Experimental test results

Figure 6 shows the experimental test results with respect to the center-to-center spacing of the cylinders at the wind azimuth of  $0^\circ$  (i.e. two cylinders are in a tandem arrangement in the direction of the wind). The root mean square (rms) displacements are normalized by dividing them by the diameter of a cylinder. In the results of the parallel cylinder model test of  $3D$  spacing (see figure 6(a)), the amplitude of the horizontal vibration is higher than that of the vertical vibration at the wind speed of  $4.7$  m s<sup>-1</sup>. On the other hand, the horizontal vibration gradually decreases with the increase in wind speed and it finally vanishes at a wind speed of  $8.6$  m s<sup>-1</sup>, when the vertical vibration suddenly governs the motion of the cylinder. This type of wake galloping is sometimes called ‘wake galloping with unstable slope’. In the results of the parallel cylinder model test of  $4D$ – $6D$  spacing (see figures 6(b)–(d)), the vertical vibration gradually increases with the increase in wind speed. This type of wake galloping is sometimes called ‘wake galloping with stable slope’. The onset speeds of the vertical vibrations in the parallel cylinder model test of  $4D$ – $6D$  spacing are lower than that for  $3D$  spacing. In the case of the parallel cylinder model test of  $7D$  spacing (see figure 6(e)), the vertical vibration occurs at a wind speed of  $7$  m s<sup>-1</sup>, then gradually the amplitude of vibration decreases with the increase in wind speed, such as the vortex-induced vibration. In the cases of the

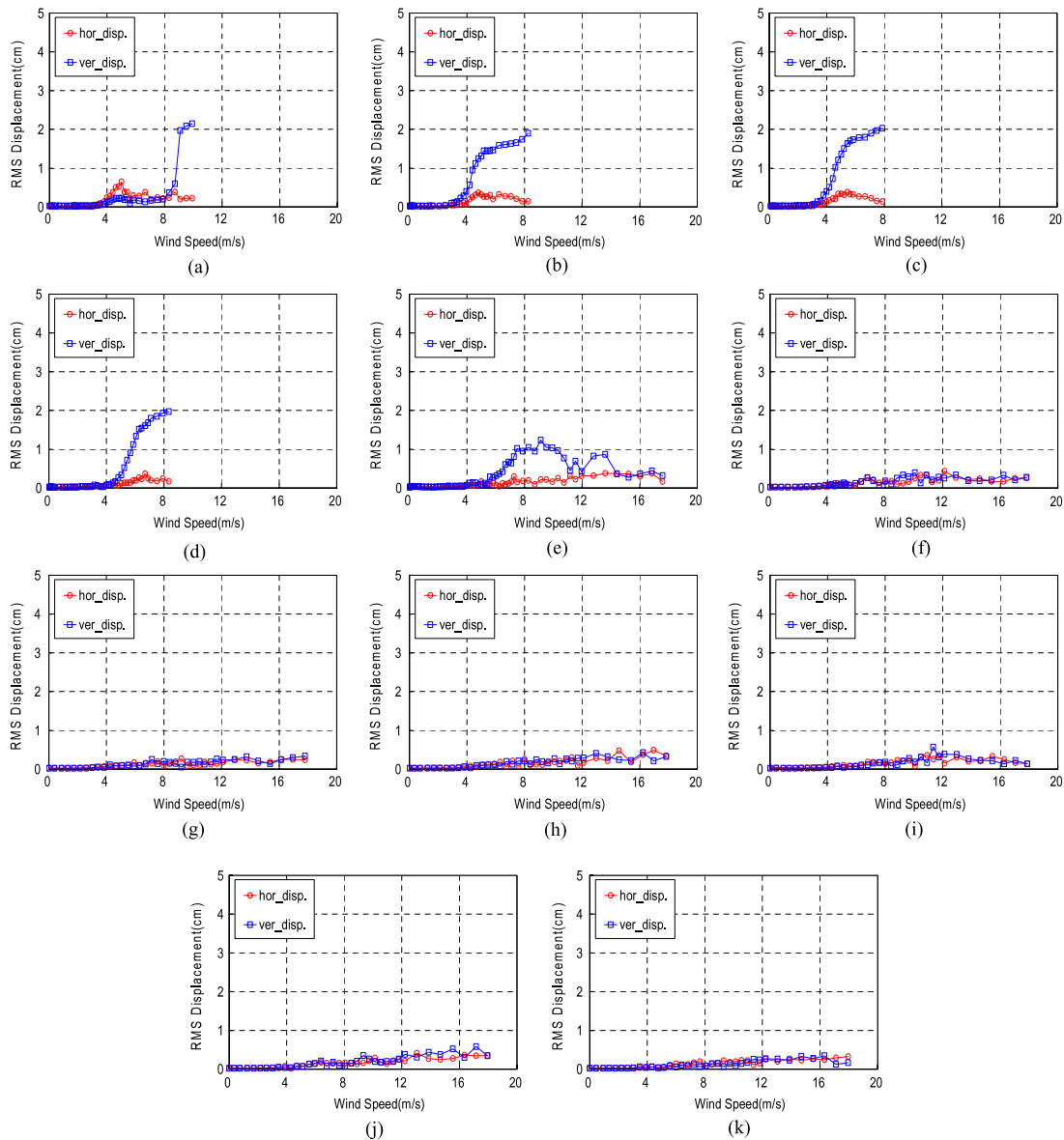


**Figure 6.** Results of parallel cylinder model test (spacing:  $3D$ – $13D$ ); (a)  $3D$ , (b)  $4D$ , (c)  $5D$ , (d)  $6D$ , (e)  $7D$ , (f)  $8D$ , (g)  $9D$ , (h)  $10D$ , (i)  $11D$ , (j)  $12D$  and (k)  $13D$ .

parallel cylinder model tests over  $8D$  spacing (see figures 6(f)–(k)), there are no distinguishable vibrations except for small buffeting responses.

It is known that the oscillation of a body with gradually increasing amplitude at relatively low wind speed is appropriate for energy harvesting. Therefore, the parallel cylinder models of  $4D$ – $5D$  spacing could be considered to be appropriate for an energy harvesting system based on the wake galloping phenomenon.

#### 2.4. Summary

According to the wind tunnel test conducted in this study, several characteristics of the wake galloping phenomenon are observed as follows:

- (1) The spacing of the cylinders is one of the most important parameters which governs the characteristics of wake

galloping and it can be said that notable wake galloping occurs between  $3D$  to  $6D$  spacing. In the case of approximately  $3D$  spacing of the cylinders, a drastic increase in vibration may occur, and this type of wake galloping is sometimes called ‘wake galloping with unstable slope’. In the cases of  $4D$ – $6D$  spacing, on the other hand, the amplitude of vibration increases gradually, and this type of wake galloping is sometimes called ‘wake galloping with stable slope’.

- (2) The amplitude of wake galloping may vary depending on specific conditions such as structural properties, flow properties and wind directions. In the cases of  $3D$ – $6D$  spacing, the amplitudes become larger as the wind gets faster. However, there is no disruptive increase of amplitude in those cases. According to previous research [18], moreover, it was observed that the maximum amplitude of wake galloping cannot exceed

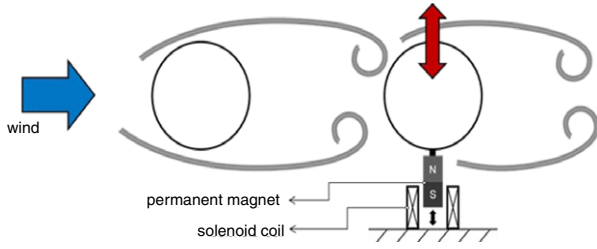


**Figure 7.** Schematic of the proposed energy harvesting device.

three times the cylinder diameter, because the instability caused by the wake interference decreases when the relative angle for wind on the parallel cylinder increases. The test results match well with the observations in [18].

- (3) In the case of two cylinders in a tandem arrangement in the direction of the wind, the cross-wind vibration might be dominant.
- (4) The wake galloping phenomenon occurs at a relatively low wind speed, compared to other divergent oscillation phenomena, and it remains within a wide range of wind speeds. These observations agree with previous research [18].

### 3. Proposed energy harvesting system using wake galloping

According to the wind tunnel test results shown in the previous section, it has been clearly validated that the wake galloping phenomenon has several promising characteristics for extracting wind energy. Therefore, a new class of energy harvesting devices based on this phenomenon is proposed by using Faraday's law of electromagnetic induction. That is, an electromagnetic system consisting of a permanent magnet and a solenoid coil is attached to the movable cylinder as shown in figure 7. This figure indicates the schematic of the proposed energy harvesting device. As seen from the figure, the permanent magnet attached to the rear cylinder will be easily vibrated due to the wake galloping phenomenon. At the same time, the electromotive force (i.e. the induced voltage) can be generated in the solenoid coil part located on the fixed structure.

The electromagnetic mechanism has been used to generate electricity since the 1930s. As the permanent magnet moves in and out of the solenoid coil, it generates the electromotive force (emf). In other words, it changes the kinetic energy of the relative movement between the magnet and the coil into electric energy (i.e. induced current). Based on Faraday's law of electromagnetic induction, the induced voltage (or emf) is determined as

$$\varepsilon = -\frac{d\Phi_B}{dt} \quad (1)$$

where  $\varepsilon$  is the induced emf and  $\Phi_B$  is the magnetic flux. The maximum open-circuit voltage across the coil ( $V_S$ ) can be expressed as [19]

$$V_S = NBl \frac{dy}{dt} \quad (2)$$

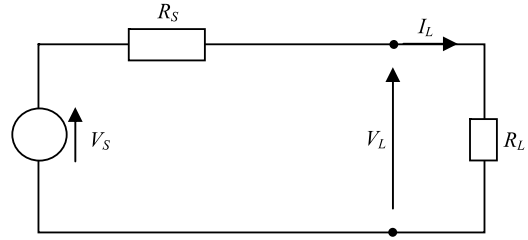


**Figure 8.** Equivalent circuit.

where  $N$  is the number of turns in the coil,  $B$  is the strength of the magnetic field,  $l$  is the mean circumference of the coil and  $y$  is the relative motion between the magnet and the coil.

An equivalent circuit of the proposed energy harvesting device can be modeled as shown in figure 8 by a Thévenin equivalent [20], with a load resistance,  $R_L$ , a source resistance,  $R_S$ , and an open-circuit voltage of the source,  $V_S$ . In the diagram, the power is being transferred from the source to a load with resistance  $R_L$ , resulting in a current  $I_L$ . By Ohm's law, the current in this circuit,  $I_L$ , is simply the source voltage divided by the total circuit resistance:

$$I_L = \frac{V_S}{(R_S + R_L)}. \quad (3)$$

Also, the voltage across the load resistor,  $V_L$ , can be calculated using the voltage divider rule as follows:

$$V_L = V_S \frac{R_L}{R_S + R_L}. \quad (4)$$

Therefore, the power supplied to the battery,  $P_L$ , can be expressed as

$$P_L = V_L I_L = I^2 R_L = \left( \frac{V_S}{R_S + R_L} \right)^2 R_L. \quad (5)$$

Note that the maximum power from the source can be obtained when the load resistance is identical to the internal source resistance (i.e.  $R_L = R_S$ ) according to the maximum power transfer theory [20].

## 4. Experimental validation of the proposed energy harvesting system

### 4.1. Experimental set-up

This section describes the experimental set-up of a wind tunnel test for validating the effectiveness of the proposed energy harvesting device. The set-up is slightly changed from the characteristic test for wake galloping described in section 2.2 by adding the energy harvesting part consisting of a permanent magnet (neodymium,  $\Phi 10 \text{ mm} \times 25 \text{ mm} \times 3 \text{ EA}$ ) attached to the end of the rear cylinder and the solenoid coil fixed to the ground. Table 2 demonstrates the detailed data of the model used. The geometric data of the model is exactly the same as in the previous test; however, the mass per unit length of the model is much smaller (i.e.  $1.539 \text{ kg m}^{-1}$  in this test versus

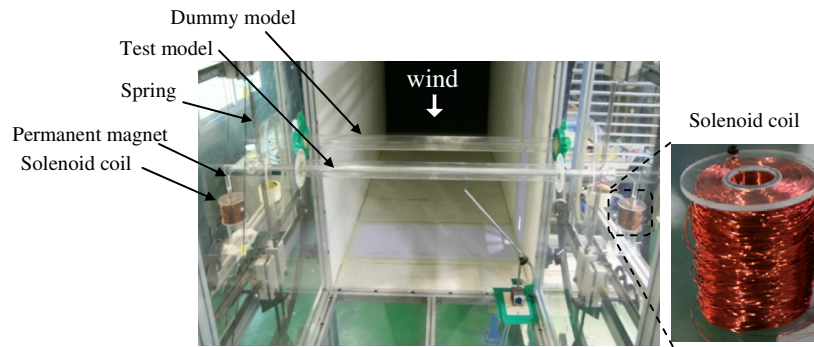


Figure 9. Test set-up in wind tunnel facility.

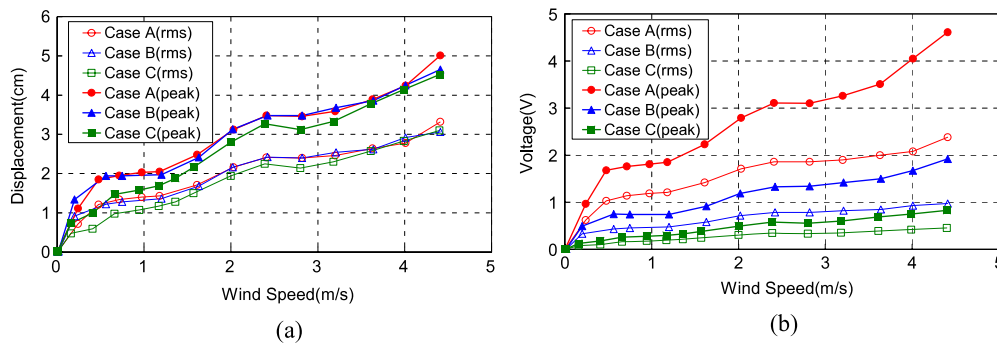


Figure 10. Test results; (a) wind speed versus amplitude and (b) wind speed versus generated voltage.

Table 2. Data of test model.

Diameter of cylinders	Length of cylinders	Mass per length	Natural frequency	Logarithmic decrement	Scruton number
5 cm	0.85 m	1.539 kg m <sup>-1</sup>	1.95 Hz	$\delta = 0.005$	5.0

8.184 kg m<sup>-1</sup> in the previous test). That is why the natural frequency in this test is slightly larger than that in the previous test. The spacing of the model is selected at  $5D$  because this value has the optimal performance according to the wake galloping characteristic test. The mass of the model and the damping ratio of the system are set up as low as possible, so that the onset velocity of the phenomenon is low. Figure 9 shows the photo of the test set-up in the wind tunnel facility.

Table 3 shows the test cases conducted in this study. As shown in the table, the test will be carried out in two steps. In the first test, three cases are considered with different coil types (i.e. cases A, B and C). Each coil type has the same volume. The number of turns is a main design parameter in this test. As seen from table 3, there are three different values for this parameter (i.e. 2770, 1264 and 580) by using three different wire diameters (i.e. 0.4, 0.8 and 1.2 mm). Note that, if the wire in the coil is thin, then the number of turns is large (case A); on the other hand, if the wire is thick, then the number of turns is small (case C). In the second test, the natural frequency of the model is changed by replacing springs from 1.95 to 4.80 Hz (i.e. cases B-1, B-2 and B-3 in table 3).

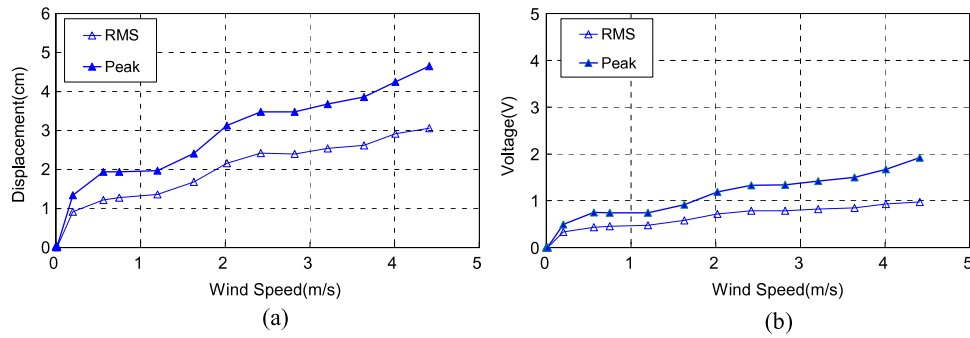
Table 3. Test cases.

Case	Coil type	Natural frequency (Hz)
A	-No. of turns = 2770 -Wire diameter = 0.4 mm -Resistance = 48.8 $\Omega$	1.95
B (B-1)	-No. of turns = 1264	1.95
B-2	-Wire diameter = 0.8 mm	2.95
B-3	-Resistance = 7.0 $\Omega$	4.80
C	-No. of turns = 580 -Wire diameter = 1.2 mm -Resistance = 1.4 $\Omega$	1.95

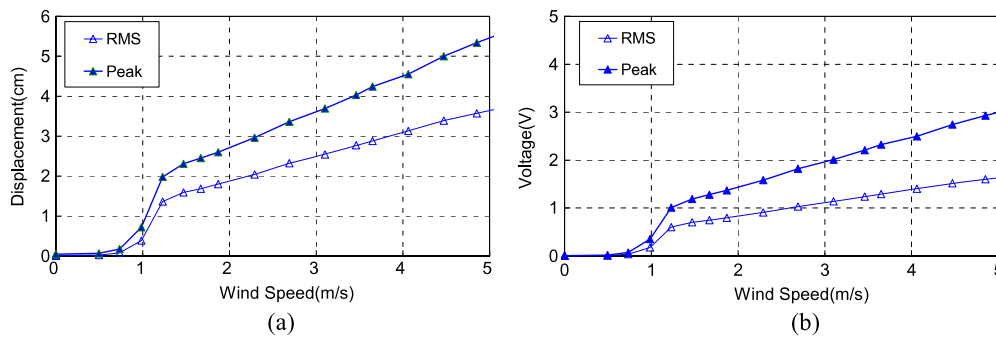
#### 4.2. Experimental test results

Figure 10 shows the experimental test results according to different wire diameters (i.e. cases A–C). In each case, the rms and peak displacement and the corresponding voltage responses are measured. The peak displacements are always slightly larger than the rms ones. Figure 10(a) shows that, as the wind speed increases, the vibration amplitude of the rear cylinder gradually increases. This monotonic increase of the response with respect to wind speed was reported by





**Figure 11.** Test results in case B-1; (a) wind speed versus amplitude and (b) wind speed versus generated voltage.



**Figure 12.** Test results in case B-2; (a) wind speed versus amplitude and (b) wind speed versus generated voltage.

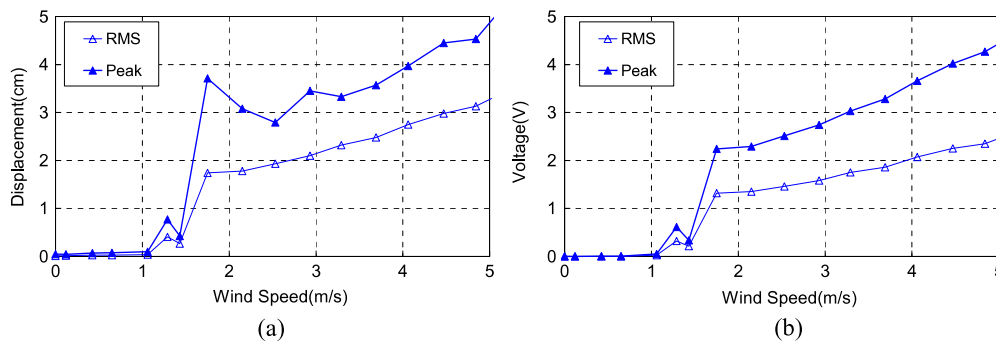


**Figure 13.** Test results in case B-3; (a) wind speed versus amplitude and (b) wind speed versus generated voltage.

Korkischko and Meneghini [21]. Also, it is observed from the figure that the vibration amplitudes in all cases are nearly the same, regardless of the variation in wire diameters. It is expected that the device can generate electricity for a wide range of wind speeds. On the other hand, the generated voltages from the electromagnetic part are very changeable as shown in figure 10(b). The figure indicates that, if the number of turns decreases, the generated voltage is drastically decreased.

Table 4 represents the electric power generated from the device, which is calculated based on equation (5). As seen from the table, the generated power increases gradually, as the wind speed gets faster in all cases. Also, at the same wind speed, the generated power in case C is larger than that in the other two cases (cases A and B). That is because the impedance (i.e. the resistance) of the system in the case with the small wire diameter coil (i.e. case A) is much larger than that in the case

**Table 4.** Average power generated from the energy harvesting device (calculated).

Wind speed ( $\text{m s}^{-1}$ )	Average power (mW)		
	Case A	Case B	Case C
2.5	32.3	39.3	43.8
3.5	45.4	54.0	61.1
4.5	58.5	68.7	78.4

with the large wire diameter coil (i.e. case C) as seen from table 3.

In order to improve the efficiency of the energy harvesting device, its natural frequencies are increased by replacing the springs with harder ones in figure 10 (i.e. cases B-1, B-2 and B-3 in table 3). The other parameters of the system are the same as those in case B. Figures 11–13 represent

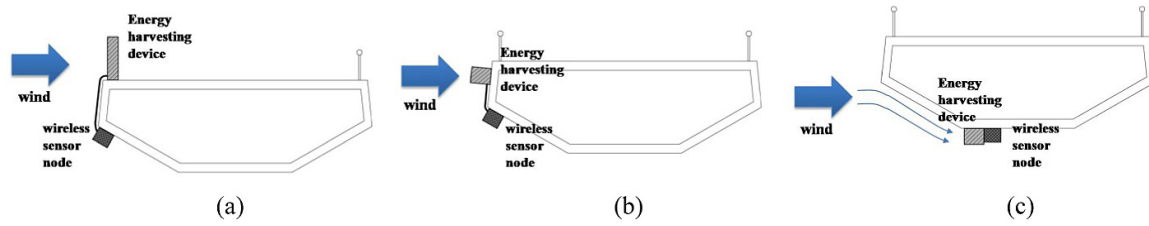


**Figure 14.** Possible installation locations for the energy harvesting device on a bridge; (a) case 1, (b) case 2 and (c) case 3.

**Table 5.** Average power generated from the energy harvesting device (calculated).

Wind speed ( $\text{m s}^{-1}$ )	Average power (mW)		
	Case B-1	Case B-2	Case B-3
2.5	39.3	69.2	173.8
3.5	54.0	102.3	272.1
4.5	68.7	135.4	370.4

the experimental test results. It is first observed from figures 11(a), 12(a) and 13(a) that the onset speed of wake galloping is increased as the natural frequency of the device is increased. This is the typical characteristic of aerodynamic instability phenomena. It is also observed from the figures that there is a vibration with finite amplitude for a wide range of wind speeds. Figures 11(b), 12(b) and 13(b) demonstrate the results of the corresponding induced voltage with respect to the natural frequencies of the device. It is observed that all the responses (i.e. displacement amplitude and generated voltage) show a monotonic increase as the wind speed increases [21]. In particular, as the natural frequencies get higher, the responses show an almost linear increase. That might be because the test model is more completely vibrated in the vertical direction due to its support springs with higher stiffness. Table 5 shows the harvested average power with different natural frequencies, which are the values calculated using equation (5). As seen from the table, the amount of generated power can be increased as the wind speed gets faster or the natural frequency gets larger. According to the test results, therefore, the best energy harvesting case is case A-3 (i.e. a natural frequency of 4.8 Hz and a wind speed of  $4.5 \text{ m s}^{-1}$ ).

#### 4.3. Discussion on its applicability to civil engineering structures

As shown in section 3, the prototype proposed energy harvesting device could generate about 370 mW under a wind speed of  $4.5 \text{ m s}^{-1}$ . In this section, the applicability of the system to real civil engineering structures (e.g. cable-stayed bridges) is extensively discussed based on the measured wind information around the bridge site in Korea. First, possible locations for the proposed energy harvesting device for generating electricity and providing it to a wireless sensor node in a bridge under wind load are described in figure 14. As shown in figure 14(a), it can also be used as a bridge rail on the bridge because its energy harvesting performance is not affected by the vertical installation. Also, the device can be

**Table 6.** Mean wind speed at bridge site and expected output power from the device.

Data type	Mean wind speed ( $\text{m s}^{-1}$ )	Output power from the device (estimated) (mW)
Data from KMAC	5.3	About 450
Data measured at the bridge site	4.3	About 350

placed on the side as well as the bottom of the bridge deck as shown in figures 14(b) and (c), respectively.

For validation of the applicability of the proposed device to bridge structures, a cable-stayed bridge (the second Jindo Bridge) located in Korea is considered. According to the records from the Korean Meteorological Administration Center (KMAC) [22], the average wind speed around the bridge site for the last five years is about  $5.3 \text{ m s}^{-1}$ . Also, the one-day mean wind speed, which was measured on the bridge deck by our research group, was about  $4.3 \text{ m s}^{-1}$  [22]. Based on these actual data, it is known that case B-3 (i.e. wind speed of  $4.5 \text{ m s}^{-1}$ ) in the tests is not a severe wind condition, but a moderate one. By combining these actual wind data and the previous wind tunnel test results, the generated power from the device can be expected as in table 6.

In order to verify whether it is possible to use the harvested energy from the proposed energy harvesting device as the input energy for wireless sensor nodes, the test results of the estimated power consumption of Imote2, which is a commercially available wireless sensor platform for structural health monitoring, is considered [22, 23]. According to Park *et al* [22], when two sensing processes are carried out per day by a wireless sensor node, about 42 mWh of power is required. Assuming that a wind blows around the bridge site at a speed of  $4.5 \text{ m s}^{-1}$  for an hour per day and a rechargeable battery with 75% efficiency is used for storage of the harvested energy (i.e. 25% of the harvested energy may be lost during the charging process of the voltage), electrical energy of about 267 mWh can be stored in the rechargeable battery. It is also assumed that about 90% of the stored energy can be consumed for powering Imote2 sensor nodes. Finally, the total energy to be used for sensor nodes is about 240 mWh. This, in the case that the sensing process by an Imote2 sensor node is carried out twice per day, the sensor node can be operated for more than 5 days. It is, therefore, concluded that the energy harvesting capability of the proposed device could be utilized as a power source for wireless sensor nodes.

## 5. Conclusions

In this paper, the experimental investigation of a wake-galloping-based electromagnetic energy harvesting device is extensively carried out. To this end, the characteristics and mechanisms of various aerodynamic instability phenomena are examined first. Then, a wind tunnel test is carried out in order to more clearly understand the occurrence condition of the selected aerodynamic instability phenomenon (i.e. wake galloping). Based on the wind tunnel test results, a prototype electromagnetic energy harvesting device is designed and manufactured. By using the prototype device, the effectiveness of the proposed system is verified with different parameters through the wind tunnel test. As seen from the test results, one can obtain an average generated power of 50–370 mW under a wind speed of 2.5–4.5 m s<sup>-1</sup>. In the proposed system, moreover, electromagnetic induction can be easily increased. That is, much larger generated power can be expected. It is, therefore, clearly seen that the applicability of the proposed energy harvesting system using the wake galloping phenomenon is experimentally verified, and it could be effectively used as a power supply for providing the electricity to wireless sensor nodes in a bridge under moderate wind conditions. A field test at the bridge site is now underway.

## Acknowledgment

The authors gratefully acknowledge the support of this research by the KAIST Institute funded by the Korean Ministry of Education, Science and Technology.

## References

- [1] Duncan J W 1948 *The Fundamentals of Flutter* (London: ARC/R&M) pp 1–36
- [2] McKinney W and DeLaurier J 1981 The wingmill: an oscillating-wing windmill *J. Energy* **5** 109–15
- [3] Jones K, Platzer M F and Davis S 1999 Oscillating-wing power generator *Proc. of ASME/JSME FEDSM'99*
- [4] Isogai K, Yamazaki M, Matsubara M and Asaoka T 2003 Design study of elastically supported flapping wing power generator *Proc. Int. Forum on Aeroelasticity and Structural Dynamics*
- [5] Ertuk A, Bilgen O, Fontenille M and Inman D J 2008 *Proc. ICAST 2008 (Ascona)*
- [6] Ertuk A, Vieira W G R, De Marqui C Jr and Inman D J 2010 On the energy harvesting potential of piezoaeroelastic systems *Appl. Phys. Lett.* **96** 184103
- [7] Bryant M and Garcia E 2009 *Proc. SPIE* **7288** 728812
- [8] Bryant M and Garcia E 2009 *Proc. SPIE* **7493** 74931W
- [9] Dikson R M 2008 *New Concepts in Renewable Energy* <http://newrenewables.net/>
- [10] Li S and Lipson H 2009 Vertical-stalk flapping-leaf generator for wind energy harvesting *Proc. ASME 2009 Conf. on Smart Materials, Adaptive Structures and Intelligent Systems*
- [11] Li S, Yuan J and Lipson H 2011 Ambient wind energy harvesting using cross-flow fluttering *J. Appl. Phys.* **109** 026104
- [12] St Clair D, Bibo A, Sennakesavababu V R, Daqaq M F and Li G 2010 A scalable concept for micropower generation using flow-induced self-excited oscillations *Appl. Phys. Lett.* **96** 143103
- [13] Matsumoto M, Okubo K, Ito Y, Matsumiya H and Kim G 2005 Fundamental study on the efficiency of flutter power generation system *Proc. 19th National Symp. on Wind Engineering* pp 151–6
- [14] Matsumoto M 2005 Flutter instability of structures *The Fourth European and African Conf. on Wind Engineering* pp 6–11
- [15] Jung H J, Lee S W and Jang D D 2009 Feasibility study on a new energy harvesting electromagnetic device using aerodynamic instability *IEEE Trans. Magn.* **40** 4376–79
- [16] Kim H 2009 Mechanism of wake galloping of two circular cylinders *Doctoral Dissertation* Department of Civil Engineering at Nagoya University, Nagoya, Japan
- [17] Davenport A G 1962 Buffeting of a suspension bridge by storm winds *J. Struct. Division ASCE* **88** 233–68
- [18] Public Works Research Institute 1995 *Manual of Aerodynamic Countermeasure Against Wake Galloping*
- [19] Inman D J and Priya S 2009 *Energy Harvesting Technologies* (New York: Springer Science +Business Media, LLC)
- [20] [http://en.wikibooks.org/wiki/Circuit\\_Theory/Maximum\\_Power\\_Transfer](http://en.wikibooks.org/wiki/Circuit_Theory/Maximum_Power_Transfer)
- [21] Korkischko I and Meneghini J R 2010 Experimental investigation of flow-induced vibration on isolated and tandem circular cylinders fitted with strakes *J. Fluids Struct.* **26** 611–25
- [22] Park J W, Jung H J, Jo H K, Jang S and Spencer B F Jr 2010 Feasibility study of wind generator for smart wireless sensor node in cable-stayed bridge *Proc. SPIE Conf. on Sensors and Smart Structures Technologies for Civil, Mechanical and Aerospace Systems (San Diego, CA)*
- [23] Jang S, Jo H K, Cho S, Mechtov K, Rice J A, Sim S H, Jung H J, Yun C B, Spencer B F Jr and Agha G 2010 Structural health monitoring of a cable-stayed bridge using wireless smart sensor technology: deployment and evaluation *Smart Struct. Syst.* **6** 439–59